Neuron
Article

Neural Mechanisms of Speed-Accuracy Tradeoff

Richard P. Heitz[1,*] and Jeffrey D. Schall[1]
[1]Center for Integrative & Cognitive Neuroscience, Vanderbilt Vision Research Center, Department of Psychology, Vanderbilt University, Nashville, TN 37240, USA
*Correspondence: richard.p.heitz@vanderbilt.edu
http://dx.doi.org/10.1016/j.neuron.2012.08.030

SUMMARY

Intelligent agents balance speed of responding with accuracy of deciding. Stochastic accumulator models commonly explain this speed-accuracy tradeoff by strategic adjustment of response threshold. Several laboratories identify specific neurons in prefrontal and parietal cortex with this accumulation process, yet no neurophysiological correlates of speed-accuracy tradeoff have been described. We trained macaque monkeys to trade speed for accuracy on cue during visual search and recorded the activity of neurons in the frontal eye field. Unpredicted by any model, we discovered that speed-accuracy tradeoff is accomplished through several distinct adjustments. Visually responsive neurons modulated baseline firing rate, sensory gain, and the duration of perceptual processing. Movement neurons triggered responses with activity modulated in a direction opposite of model predictions. Thus, current stochastic accumulator models provide an incomplete description of the neural processes accomplishing speed-accuracy tradeoffs. The diversity of neural mechanisms was reconciled with the accumulator framework through an integrated accumulator model constrained by requirements of the motor system.

INTRODUCTION

The speed-accuracy tradeoff (SAT) is a strategic adjustment in the decision process adapting to environmental demands exhibited by humans (Fitts, 1966; Wickelgren, 1977; Bogacz et al., 2010) as well as rats (Kaneko et al., 2006), bees (Chittka et al., 2003), and ant colonies (Stroeymeyt et al., 2010). Computational decision models explain SAT in terms of a stochastic accumulation of noisy sensory evidence from a baseline level over time; responses are produced when the accumulated evidence for one choice reaches a threshold. Elevating the decision threshold (or reducing the baseline) produces slower, more accurate responses; lowering the threshold (or raising the baseline) produces faster, less accurate responses.

Recent neuroimaging studies have presented evidence consistent with these predictions, suggesting a parallel between stochastic accumulator models and neural processing (Forstmann et al., 2008, 2010; Ivanoff et al., 2008; van Veen et al., 2008; Mansfield et al., 2011; van Maanen et al., 2011). However, the neurophysiological mechanisms accomplishing SAT are unknown, as no test of SAT adjustments in nonhuman primates has been reported. Only neurophysiology provides the spatial and temporal resolution necessary to decisively test the implementation of computational decision models. Multiple laboratories have demonstrated how the stochastic accumulation process is instantiated through the activity of specific neurons in the frontal eye field (FEF; Hanes and Schall, 1996; Boucher et al., 2007; Woodman et al., 2008; Purcell et al., 2010, 2012; Ding and Gold, 2012), lateral intraparietal area (LIP; Roitman and Shadlen, 2002; Wong et al., 2007), superior colliculus (SC; Ratcliff et al., 2003; 2007), and basal ganglia (Ding and Gold, 2010). However, no study has investigated whether single neurons accomplish SAT as predicted by the models. We addressed this by training macaque monkeys to perform voluntary, cued adjustments of SAT during visual search while recording from single neurons in the FEF.

Monkeys exhibited proactive and immediate changes in behavior when SAT cues changed. As observed in human SAT, an accumulator model described their behavioral data with systematic variation of just one parameter between SAT conditions—decision threshold. However, the neural correlates of SAT were much more diverse, affecting preperceptual, perceptual, categorical, and premovement activity in distinct functional types of neurons. Moreover, although the accumulator models exhibit greater excursions from baseline to threshold when accuracy is stressed relative to speed, the neurons that have been identified most clearly with stochastic accumulation exhibited smaller excursions. Thus, these results demonstrate that the simple stochastic accumulator model framework provides an incomplete description of the brain processes mediating SAT.

These discrepancies were reconciled by recognizing constraints of the brainstem circuitry generating the saccades, which had invariant dynamics across all SAT conditions. These constraints require that the final net influence of FEF movement neurons is equivalent across SAT conditions. Our data were consistent with this; we discovered that leaky integration of FEF movement neuron activity terminated at the same level across SAT conditions. These relationships led naturally to an integrated accumulator model that reconciles the key features of stochastic accumulator models with the variety of neural adjustments we observed during SAT.

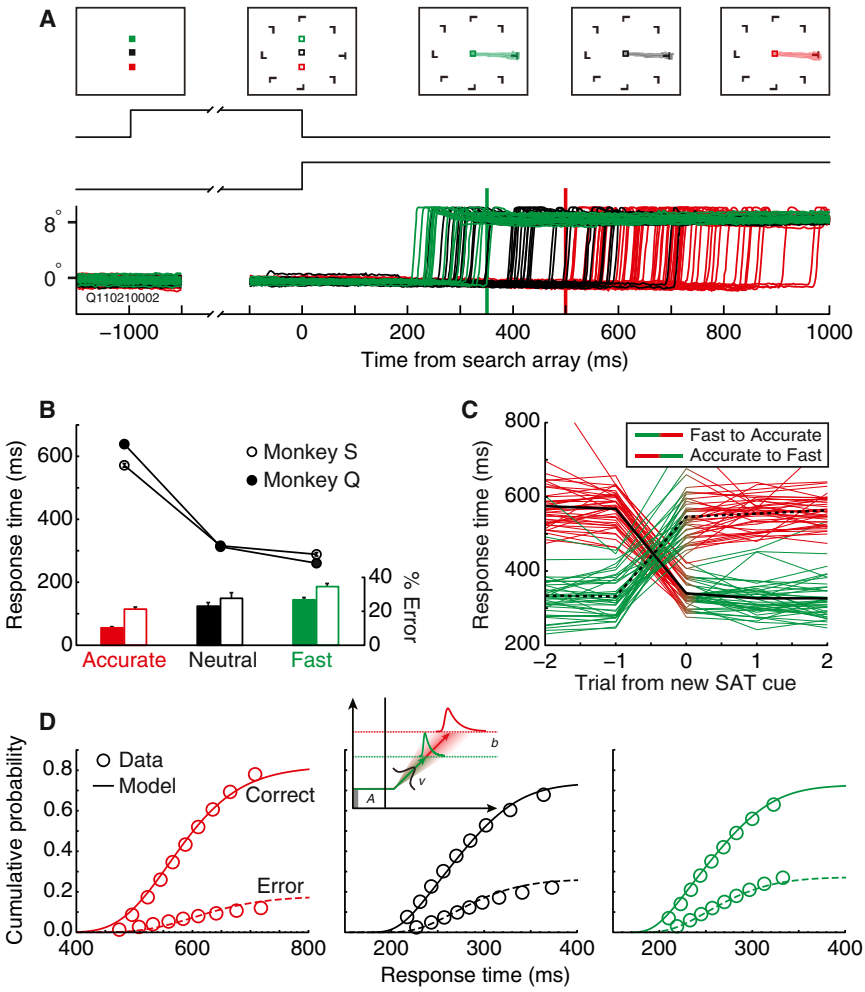

Figure 1. Speed-Accuracy Manipulation of Visual Search Performance

(A) Trials began with a fixation cue signifying whether the trial was to be Fast (green), Accurate (red), or Neutral (black). Monkeys searched for a target item (rotated T or L) presented with seven distractors (rotated L or T). In some sessions, distractors were of homogeneous orientation; in other sessions, they were randomly rotated. Eye position plotted for correct trials in a session illustrates the effect of the cue on RT. Vertical lines indicate response deadlines for Fast (green) and Accurate (red) conditions for this session.

(B) Mean RT and accuracy rate across all sessions for each monkey. RT decreased and error rate increased with speed stress in both monkeys (monkey Q RT: $t_{24} = -19.4$, accuracy: $t_{24} = -11.1$; monkey S RT: $t_{14} = -13.7$, accuracy: $t_{14} = -5.6$, all $p < 0.001$, linear regression). Vertical bars show ±1 SE.

(C) Mean RT on trials before and after change of SAT cue. Data from all sessions are plotted with each session contributing two lines, one for Fast to Accurate (green to red) switches and one for Accurate to Fast (red to green). RT increased immediately and significantly between Fast and Accurate blocks (two-tailed $t_{39} = -20.3$, $p < 0.001$) and decreased between Accurate and Fast blocks ($t_{39} = 30.3$, $p < 0.001$). Data from the Neutral condition are not displayed.

(D) Accumulator model fits for Accurate (left), Neutral (middle), and Fast (right) conditions. Observed (circles) and predicted (lines) defective cumulative probability of correct (solid) and error (dashed) RTs for all trials sampled are shown. Only threshold varied across conditions; other parameters were shared (inset).

RESULTS

Assessing Speed-Accuracy Tradeoff in Visual Search

Two *Macaca radiata* (Q and S) performed a visual search task to locate a target item presented among distractor items (T or L among Ls or Ts; Figure 1A). Each trial began when monkeys fixated a central point, the color of which cued one of three SAT conditions—Accurate, Neutral, or Fast. SAT conditions were presented in blocks of 10–20 trials. Besides fixation point color, the conditions employed several reward (juice) and punishment (time out) contingencies (Experimental Procedures). The Accurate and Fast conditions were enforced with response deadlines similar to some human studies (Rinkenauer et al., 2004; Heitz and Engle, 2007), adjusted so that ~20% of trials would be too fast after Accurate or too slow after Fast cues. Reward and time outs were jointly determined both by response accuracy and response time (RT) relative to the deadlines. Through extensive training, monkeys learned to adopt three different cognitive sets cued by fixation point color. While response deadlines were crucial in training and retaining the SAT, they were not necessary in the short term; both monkeys maintained RT adjustments without the deadline contingencies.

After training, monkeys were tested in 40 experimental sessions (25 from monkey Q, 15 from monkey S). Both monkeys demonstrated a pronounced SAT in every session, characterized by decreasing RT and accuracy with increasing speed stress (Figure 1B). Also, both monkeys responded to SAT cue changes with an immediate adjustment rather than a slow discovery of reinforcement contingencies; RT increased or decreased significantly on the first trial of a block switch (Figure 1C, see Movie S1 available online). These observations demonstrate the voluntary and proactive behavioral adjustments monkeys produced.

Accumulator Models Explain Monkey SAT with a Change in Decision Threshold

Human performance in decision-making tasks has been explained as a stochastic accumulation of evidence (Ratcliff and Smith, 2004). Accumulator models explain SAT by a change in the decision threshold or equivalently the baseline (reviewed by Bogacz et al., 2006). Relative to a Neutral condition, lowering the decision threshold promotes faster but more error-prone responses, whereas raising the threshold promotes slower and more accurate responses. To determine whether the monkey

Table 1. Linear Ballistic Accumulator Parameter Estimates

Data Set	Baseline (*A*)	Threshold (*b*)			Drift Rate (*v*)	Nondecision Time (T_0)
		Accurate	Medium	Fast		
Monkey S (sessions)	30 ± 8.1	277 ± 4.2	144 ± 14.4	135 ± 4.7	0.55 ± 0.01	81 ± 8.4
Monkey Q (sessions)	64 ± 8.1	320 ± 4.0	121 ± 10.7	105 ± 4.9	0.59 ± 0.01	138 ± 7.1
Population	85	325	149	141	0.57	101

Best-fitting parameters for LBA model with baseline (*A*), drift rate (*v*), and nondecision time (T_0) shared and threshold (*b*) variable across SAT conditions. Session fits are the mean ± SE of parameter values estimated separately for each session for a given monkey. Population fit is estimated across all trials, sessions, and monkeys. Units for *A*, *b*, arbitrary units of activation; *v*, activation/ms; T_0, ms.

SAT performance accords with this, we fit performance with the Linear Ballistic Accumulator (LBA; Brown and Heathcote, 2008). This model has been used extensively to address SAT in humans (Forstmann et al., 2008; Ho et al., 2012). LBA differs from accumulator models that include within-trial variability in the accumulation process but leads to equivalent conclusions (Donkin et al., 2011b). Consistent with previous research, the variation of performance across SAT conditions was fit best only with variation of threshold (Figure 1D; Table 1). Moreover, the best-fitting models exhibited the predicted ordering of threshold from highest in the Accurate condition to lowest in the Fast. Model variants without threshold variation across SAT conditions produced considerably poorer fits (Figure S1). Thus, the SAT performance of monkeys, as humans, can be explained computationally as a change of decision threshold in a stochastic accumulation process.

Neural Correlates of Speed-Accuracy Adjustment

Although accumulator models explain SAT with one parameter adjustment, we discovered that SAT is accomplished through multiple adjustments in the activity of visual, visuomovement, and movement neurons in FEF including (1) baseline activity before the array appeared, (2) visual response gain, (3) target selection duration, and (4) magnitude of movement activity.

We will first describe SAT adjustments in visually responsive neurons that increase firing rate when contextually salient items appear in their receptive field (RF); considering data from visual and visuomovement neurons individually or collectively did not change the results. Many previous studies have shown that these neurons signal the evolving representation of search stimulus salience (Thompson et al., 1996; Sato et al., 2001; Sato and Schall, 2003). Besides FEF (Ogawa and Komatsu, 2006; Lee and Keller, 2008; Schafer and Moore, 2011), this representation is distributed among neurons in posterior parietal cortex (Gottlieb et al., 1998; Constantinidis and Steinmetz, 2005; Ipata et al., 2006; Buschman and Miller, 2007; Thomas and Paré, 2007; Balan et al., 2008; Ogawa and Komatsu, 2009), SC (McPeek and Keller, 2002; Shen and Paré, 2007; Kim and Basso, 2008; White and Munoz, 2011), substantia nigra pars reticulata (Basso and Wurtz, 2002), and ocular motor thalamic nuclei (Wyder et al., 2004). These neurons represent the evidence on which the decision is based.

We found three adjustments of visual activity. First, SAT cues induced a shift of baseline firing rates preceding array presentation. Across the population of visual salience neurons (n = 146), 54% demonstrated significant SAT-related variability in baseline firing rate. For most (n = 65), spike rate increased after the Fast cue and decreased after the Accurate cue (Figures 2A and S2A). Baseline activity discriminated SAT conditions within 300 ms after fixating the central cue (Figure 2A, inset), and the baseline shift emerged immediately after SAT cues changed (Figure 2B), mirroring the flexibility of behavioral adaptation. Interestingly, the effect was cell specific. Neurons with and without baseline modulation were recorded within single sessions and even single electrode penetrations. Thus, SAT is accomplished in part through an immediate adjustment of cognitive set before stimuli are presented.

Second, we found evidence for adjustments of perceptual processing. Although search arrays were identical across SAT conditions, visual response magnitude increased considerably with speed stress (population average in Figure 2C; distribution in Figure S2B; note that the attenuated baseline modulation in Figure 2C is simply a consequence of averaging across neurons with and without that effect). Third, neural activity discriminated target and distractor items more quickly in the Fast condition and more slowly in the Accurate (Figure 2C). This robust effect was obtained across the population of visually responsive neurons (Figure 2D). Thus, SAT during visual search is accomplished in part through adjustments of the timing and magnitude of stimulus discrimination.

We next describe SAT adjustments in movement neurons identified with the stochastic accumulation process (Hanes and Schall, 1996; Boucher et al., 2007; Ratcliff et al., 2007; Woodman et al., 2008). Recent modeling specifies how visual neurons can provide the evidence that is accumulated by movement neurons (Purcell et al., 2010, 2012). Unlike visual neurons, movement neurons in FEF and SC project to omnipause neurons of the brainstem that are responsible for saccade initiation (Huerta et al., 1986; Langer and Kaneko, 1990; Segraves, 1992). Thus, they are uniquely poised to trigger saccades based on accumulating evidence. Movement neurons with no visual response are encountered less commonly than neurons with visual responses (Bruce and Goldberg, 1985; Schall, 1991). Here they comprised ~10% of task-related neurons (n = 14). Many more neurons had both visual responses and presaccadic movement activity (n = 70); we will present data from these separately. We found four major adjustments in movement activity. First, the baseline shift reported earlier was significant in 29% of movement neurons (Figure S2A). Second, the rate of evidence accumulation varied with SAT condition (Figures 3A and 3B). For each movement neuron separately, we fit a regression line to the accumulating discharge rate in the 100 ms

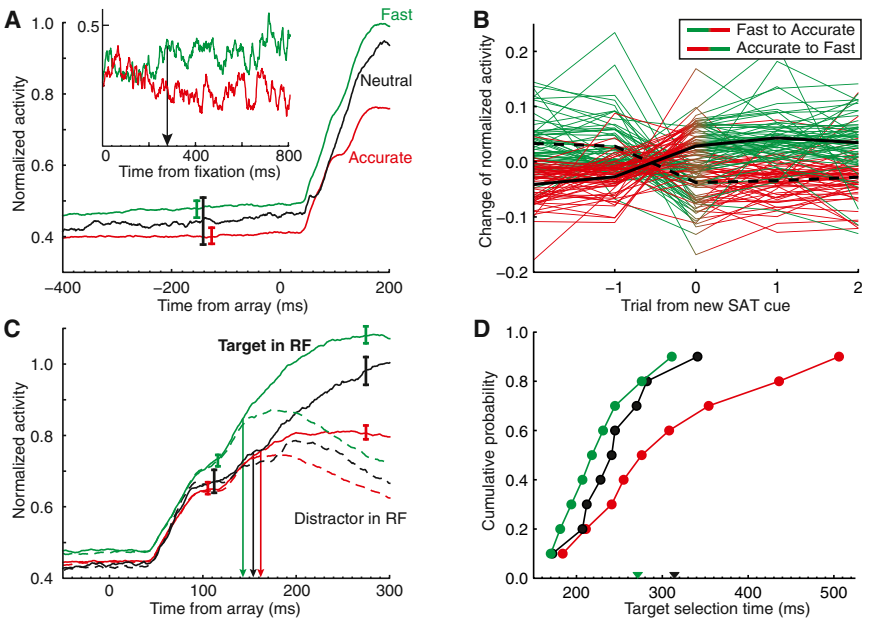

Figure 2. Adjustment of Salience Processing with SAT

(A) Average normalized activity for visual salience neurons with significantly different baseline activity in Fast versus Accurate conditions. All trials were included irrespective of upcoming target location or response. The discharge rate in the 300 ms before array presentation was significantly greater in the Fast than in the Accurate condition (t_{64} = 11.1, p < 0.001, linear regression). Vertical bars represent ±1 SE at the interval of statistical analysis. Inset shows evolution of proactive modulation after a SAT cue change; the arrow marks when the activity first signaled a change between Fast and Accurate conditions.

(B) Adjustment of baseline activity after change of SAT cue. Difference on the trials before, during, and after a SAT cue change of normalized baseline activity relative to overall average is shown. An immediate change with the presentation of a new SAT cue occurred for transitions from Accurate to Fast (two-tailed t_{64} = −10.1, p < 0.001) and from Fast to Accurate (t_{64} = 7.8, p < 0.001). Data from the Neutral condition are not displayed.

(C) Adjustment of salience processing. Average normalized discharge rates for all visual salience neurons when the target (solid) or distractors (dashed) appeared in the RF on correct trials. The baseline adjustment is less apparent because of averaging across neurons with and without the effect. Speed stress increased responsiveness (t_{144} = 7.9, p < 0.01, 100–125 ms after array; t_{144} = 9.8, p < 0.001, 250–300 ms after array, linear regression) and decreased target selection time (arrows; Accurate 162 ms > Neutral 154 ms, t_{145} = 5.1, p < 0.001; Neutral 154 ms > Fast 143 ms, t_{145} = 77.0, p < 0.001, jackknifed t tests). Vertical bars represent ±1 SE.

(D) Cumulative distribution of target selection times for all visual salience neurons. Mean RTs in the Fast, Neutral, and Accurate SAT conditions were, respectively, 271 ms (green arrowhead), 314 ms (black arrowhead), and 614 ms (beyond axis).

preceding the saccade on trials when the target was correctly located in the RF. On average, the slope was lowest in the Accurate condition, intermediate in the Neutral, and largest in the Fast condition. We observed identical effects for visuomovement neurons (Figures S3A and S3B). Third, the magnitude of movement neuron activity at saccade initiation was lowest in the Accurate condition, intermediate in the Neutral, and highest in the Fast condition (Figure 3B; visuomovement neuron activity in Figure S3B). Like baseline neural activity and mean RT, this effect emerged immediately after a change in SAT cue (Figure S2C). Thus, SAT during visual search is accomplished in part through adjustment of the magnitude of neural activity producing responses. However, this result is puzzling because the direction of the change is opposite that of accumulator models that explain SAT through decreases in threshold with increasing speed stress. We will address this in detail below. Fourth, within each SAT condition, movement neuron activity accumulated to an invariant level at saccade initiation across RT quantiles (Figures 3C–3E; visuomovement activity in Figures S3C–S3E). This replicates previous studies from multiple laboratories and tasks: when SAT is not manipulated, or when task conditions cannot be predicted or remain constant, activity at saccade does not vary with RT (Hanes and Schall, 1996; Paré and Hanes, 2003; Ratcliff et al., 2007; Woodman et al., 2008; Ding and Gold, 2012). In contrast, when conditions are precued or blocked, movement activity in FEF and SC sometimes differs (Everling et al., 1999; Everling and Munoz, 2000; Sato and Schall, 2003).

Response Time Variability, Response Withholding, Guessing, and Firing Rate Excursion Do Not Account for SAT Adjustments

We verified that these results were not confounded by simple variation of RT across conditions and that modulation in the Accurate condition was not simply a byproduct of response withholding. First, we examined activity in visually responsive and movement neurons on trials in which monkeys missed response deadlines and produced premature Accurate or late Fast responses (see Experimental Procedures). This necessarily reversed the RT effect (mean RT was faster after premature Accurate [367 ms] than late Fast [499 ms] trials, though error rates were unaffected; Figure 4A). If our results were due to RT rather than cognitive state, neural activity levels should also reverse. This did not occur; activity levels remained higher in the Fast condition than the Accurate condition for both visually responsive (Figure 4B) and movement (Figure 4C) neurons. Interestingly, we also observed that target selection time was delayed for late Fast responses relative to premature Accurate trials (Figure 4B, arrows), suggesting that response deadlines were missed due to late or premature target localization (Ho et al., 2012).

Second, we compared neural activity in the three SAT conditions holding RT constant. We matched trials from the Accurate and Fast conditions to a restricted range of RTs around the median RT in the Neutral condition (see legend to Figure 4). Once again, neural activity varied with SAT condition independent of RT (Figures 4D and 4E). Together, these results

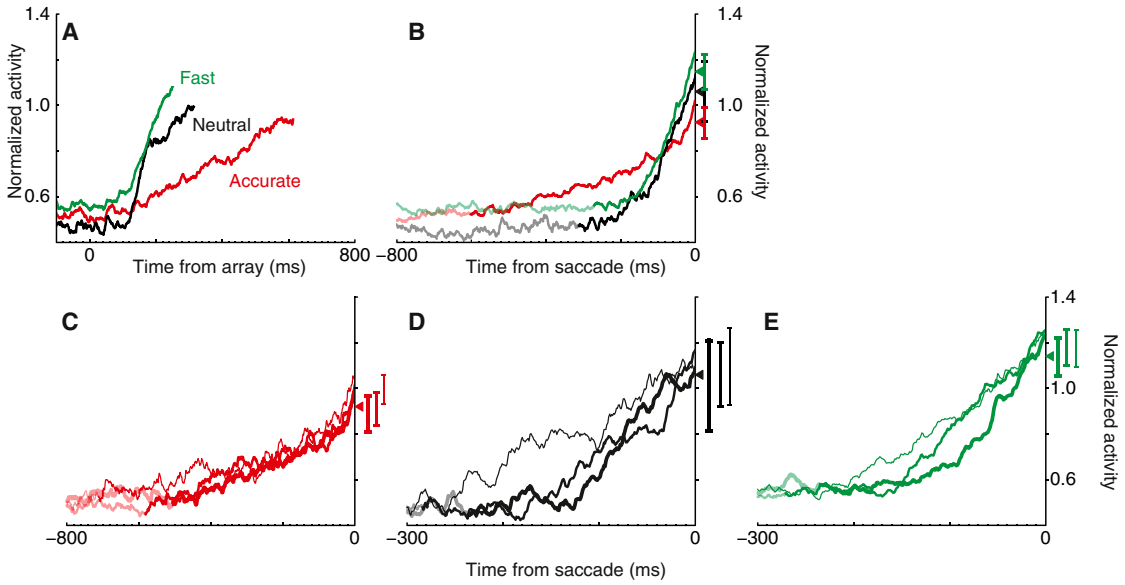

Figure 3. Adjustment of Response Preparation with SAT

(A) Average normalized discharge rate of all movement neurons for correct trials when the target fell in the neuron's movement field, aligned on array presentation. Plots are truncated at mean RT. Note that the baseline adjustment reported in text is obscured by averaging across neurons with and without the effect.

(B) Average normalized discharge rate of all movement neurons for correct trials when the target fell in the neuron's movement field, aligned on saccade initiation. Activity before mean RT is plotted lighter. On average, the slope of activity in the 100 ms preceding saccade increased with speed stress (Accurate: 2.0 < Neutral: 4.0 < Fast: 4.6 normalized sp/s^2; t_{13} = 3.1, $p < 0.01$, linear regression). Activity 20–10 ms before saccade significantly increased with speed stress (t_{13} = 2.2, $p < 0.05$, linear regression).

(C–E) Discharge rates in Accurate (C), Neutral (D), and Fast (E) conditions for correct target-in-RF trials separated into fastest (thick), intermediate (thinner), and longest (thinnest) RT quantiles. Activity 20–10 ms before saccade varied across but not within SAT conditions (all $p > 0.05$, linear regression). All vertical bars represent ±1 SE.

demonstrate that changes in cognitive state elicited by SAT cues persisted across the range of RT. In other words, fast responses in the Fast condition and equally fast responses in the Accurate condition were qualitatively different.

Were monkeys simply guessing in the Fast condition? The high accuracy rates in the Fast condition (~70%) indicate that they were not. To investigate further, we reasoned that fast guesses should result in a nonuniform distribution of errors in the Fast condition. Specifically, guesses should be more prevalent for the fastest responses than for comparably slower responses. We divided the Fast condition into RT quintiles and found that error rates differed by less than 0.3%. Further evidence against a guessing strategy is provided by our previous work showing that guesses are associated with attenuated, rather than magnified, neural activity in FEF (Heitz et al., 2010), opposite of the pattern reported here.

Some investigators have suggested that SAT is mediated not by the level of a response threshold but rather by the excursion of firing rate from baseline to threshold (Forstmann et al., 2008, 2010; van Maanen et al., 2011). We observed variation in both baseline and presaccadic activity, so it is possible that the total excursion was larger in the Accurate than Fast condition. We evaluated this by subtracting baseline firing rate (average activity in the 100 ms before the array) from presaccadic firing rate (average activity 20–10 ms before saccade) for each neuron. Contrary to this hypothesis, we found that the firing rate excursion was significantly larger in the Fast condition than the Accurate condition for the vast majority of neurons, irrespective of neuron type (Figure S4).

Leaky Integration of FEF Movement Activity Terminates at Fixed Threshold

The variety and direction of neural adjustments we observed during SAT does not correspond intuitively to the account of SAT provided by stochastic accumulator models. Reconciliation begins with the recognition that the brainstem circuitry responsible for saccade production places constraints on the form that SC and FEF movement activity can take. Stochastic accumulator models overlook these considerations because the terminal motor stage lies outside the model. This, along with a stimulus encoding stage, is captured simply by a residual time parameter. However, much is known about the anatomy, physiology, and chronometry of these afferent and efferent stages for saccades during visual search.

The following considerations demonstrate that brainstem neurons receiving movement neuron output reach a fixed level of activity across all SAT conditions when saccades are initiated. The burst neurons in the brainstem responsible for producing contraction of the extraocular muscles are gated by omnipause neurons (OPNs; Büttner-Ennever et al., 1988; Scudder et al., 2002; Kanda et al., 2007; Shinoda et al., 2008; Van Horn et al., 2010; Figure S5A). In their default state, OPNs prevent saccade generation through tonic inhibition of burst neurons; saccades are initiated precisely when this inhibition is released. Movement

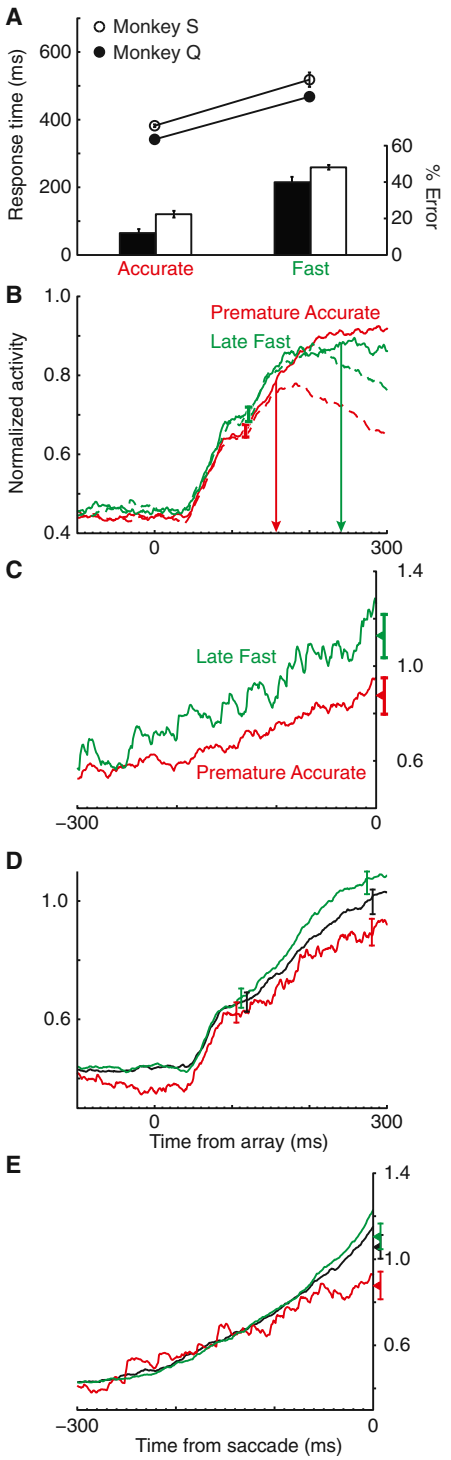

Figure 4. Experimental Controls for RT across SAT

(A) RT and error rate for missed deadlines (premature Accurate and late Fast responses). Mean RT was necessarily reversed (monkey Q $t_{24} = -5.9$, $p < 0.001$; monkey S $t_{14} = -13.2$, $p < 0.001$, two-tailed t tests), but error rate remained greater in the Fast condition (monkey Q $t_{24} = -7.6$, $p < 0.001$; monkey S $t_{14} = -10.9$, $p < 0.001$, two-tailed t tests).

(B) Average normalized activity for all visual salience neurons when the target (solid) or distractors (dashed) appeared in the RF on premature Accurate and late Fast trials (Neutral condition data are not included because there were no deadlines). Despite the reversal of RT, enhanced activity persisted 100–125 ms postarray onset in Fast compared to Accurate trials ($t_{144} = -2.8$, $p < 0.01$, two-tailed t test). Activity in a later period (250–300 ms) was not significantly different ($p > 0.05$). However, target selection time (vertical arrows) was significantly slower in late Fast (241 ms) than premature Accurate (157 ms) trials (jackknife test $t_{144} = -2{,}923.2$, $p < 0.001$).

(C) Average normalized activity for all movement neurons when the target appeared in the movement field on premature Accurate and late Fast trials. Even with the reversal of RT, movement activity 20–10 ms before saccade remained higher in late Fast than in premature Accurate trials ($t_{13} = -2.0$, $p = 0.06$, two-tailed t test).

(D) Average normalized activity for all visual salience neurons when the target appeared in the RF on Accurate, Neutral, and Fast trials equated for RT. RTs were equated by constructing a range of RTs based on ±1 SD of the median RT in the Neutral condition. RTs in Accurate, Neutral, and Fast conditions falling outside of this range were excluded, which resulted in low variability between the conditions (e.g., before correction: 614 [Accurate] – 271 [Fast] = 343 ms; after correction: 315 – 269 = 46 ms). Visual salience activity remained elevated in Fast versus Accurate trials 250–300 ms postarray onset ($t_{45} = 4.8$, $p < 0.001$, linear regression) but not in the interval 100–125 ms postarray onset ($t_{45} = 1.7$, $p = 0.10$, linear regression).

(E) Average normalized activity for all movement neurons when the target appeared in the movement field on Accurate, Neutral, and Fast trials equated for RT. Movement activity in the interval 20–10 ms prior to saccade increased with speed stress ($t_{29} = 3.1$, $p < 0.01$, linear regression). Vertical bars in all panels represent ±1 SE drawn at the interval of statistical analysis.

cells in FEF, SC, and elsewhere initiate saccades through direct, and ultimately inhibitory, projections to OPN (Raybourn and Keller, 1977; Huerta et al., 1986; Stanton et al., 1988; Segraves, 1992). Crucially, saccade velocity scales with the magnitude of OPN hyperpolarization (Yoshida et al., 1999). The invariance of saccade velocity across hundreds of milliseconds of RT variation across SAT conditions (Figure 1) entails that the level of OPN hyperpolarization must be invariant across SAT conditions.

How can the level of OPN hyperpolarization be invariant across SAT conditions if presaccadic movement neuron activity varies across SAT conditions? An answer is offered through the observation that neurons are leaky integrators. Consequently, the OPN response to FEF movement activity is a function of both its magnitude and rate of increase over time. In our data, the influence of FEF movement neurons on OPN is lower and slower in the Accurate condition and higher but briefer in the Fast condition. We reasoned that we could approximate the net inhibition onto OPN by submitting the movement neuron activity to leaky integration. For each movement neuron and each trial, activity was integrated with leak from search array presentation until saccade initiation (Experimental Procedures). The integrated value immediately before saccade initiation was indeed invariant across RT, SAT condition, and deadline accuracy (Figures 5 and S5B). The same invariance was found for visuomovement neurons (Figure S5C) but expectedly not for visual neurons. Thus, the changes observed in movement neurons across SAT conditions can translate simply into an invariant saccade trigger threshold.

An Integrated Accumulator Model Reconciles Behavioral and Neural Data

This observation motivated an alternative accumulator model architecture. Referred to as the integrated accumulator (iA), the

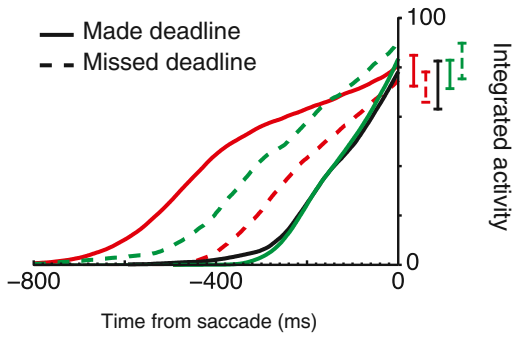

Figure 5. Leaky Integration of Movement Neuron Activity

Average activity of all movement neurons when the target appeared in the RF on correct trials, integrated with a decay constant of 100 ms from array presentation until saccade initiation. Integrated values 20–10 ms before saccade initiation were not significantly different between SAT conditions, even when the RT deadline was missed (all $p > 0.05$, linear regression). Invariance of integrated values at saccade initiation was observed with time constants of 7–167 ms. Vertical bars represent ±1 SE.

model is identical to LBA in several respects: activation functions begin at some start point and increase linearly with some drift rate. The process terminates (either correctly or incorrectly) when an accumulator reaches threshold. RT is determined by the time the threshold is reached plus some amount of time for stimulus encoding and response production, and accuracy is determined by which accumulator wins the race (Figure 6; Experimental Procedures). iA differs from LBA in two key ways. First, to capture the motor control constraints of response initiation, the linear accumulator was submitted to leaky integration and the terminal value at saccade initiation was required to be invariant across SAT conditions. Second, multiple parameters (besides threshold) could vary across SAT conditions.

The iA model reproduced both the correct and error RT distributions and accuracy rates (Figure 6). The best-fitting iA model produced the ordering of start point and drift rate parameters across SAT conditions observed in the neurons (Table 2). Thus, iA accomplishes SAT by systematically adjusting starting level (baseline) and drift rate and accounts naturally for the variation of movement neuron activity across SAT conditions.

DISCUSSION

We report the first single-neuron correlates of SAT. Monkeys performed visual search at three levels of speed stress and exhibited SAT indistinguishable from humans. Recordings from the FEF revealed distinct and diverse neural mechanisms of SAT. When accuracy was cued, baseline discharge rate was reduced before visual search arrays appeared, visual response magnitude was attenuated, neural target selection time was delayed, and movement-related activity accumulated more slowly to a lower level before saccades. The neural modulation could not be explained by guessing or procrastinating strategies. This diversity of neural mechanisms was reconciled with the stochastic accumulator model framework through an integrated accumulator model constrained by requirements of the motor system.

Stochastic Accumulator Models Provide an Incomplete Description of the Neural Mechanisms of SAT

With unprecedented resolution of the neural mechanisms mediating SAT, we found adjustments in preperceptual, perceptual, categorical, and response processes. The distinction between perceptual and response stages is beyond dispute (e.g., Miller, 1983; Osman et al., 1995; Requin and Riehle, 1995; Sato et al., 2001; Murthy et al., 2009; reviewed by Sternberg, 2001). Our results indicate that adjustments mediating SAT occur in both perceptual and response stages. Adjustments of visual responses indicated that even the representation of evidence was modulated by SAT condition, and adjustments of movement activity parallel a modulation in the accumulation process itself. Moreover, shifts of baseline discharge rate in many neurons indicated proactive changes in preparatory state. Such widespread influence of SAT has not been observed before, though previous human electrophysiological studies are consistent with a multistage locus of SAT (Osman et al., 2000; Rinkenauer et al., 2004).

The standard stochastic accumulator models of decision making account for SAT as an elevation of threshold (or excursion) to achieve greater accuracy (Bogacz et al., 2010). Other accounts suggest that SAT is achieved through an urgency signal varying the weight of sensory evidence (Cisek et al., 2009; Standage et al., 2011). However, these accounts are incomplete, as they cannot accommodate the diversity and direction of the neural adjustments we observed.

Our data are also incompatible with recent neuroimaging studies identifying SAT entirely with the excursion between accumulator baseline and threshold (Forstmann et al., 2008, 2010; Mansfield et al., 2011; van Maanen et al., 2011; Wenzlaff et al., 2011). While mathematically equivalent in some accumulator models, baseline and threshold are decisively not neurally equivalent. The independence we observed of baseline and premovement activity certainly supports this. Thus, equating baseline and threshold as a single "response caution" metric demonstrates a lack of specificity that appears important. Moreover, when we calculated firing rate excursion directly, we observed patterns still inconsistent with accumulator model predictions.

On the other hand, these neuroimaging studies have suggested that systematic modulation in medial frontal cortex contributes to SAT. This inference is consistent with neurophysiological evidence showing that weak electrical stimulation of SEF can elevate RT (Stuphorn and Schall, 2006), even though neurons in SEF do not directly control saccade initiation (Stuphorn et al., 2010; see also Scangos and Stuphorn, 2010).

This conclusion does not invalidate the models as effective parametric descriptions of performance in various tasks (Ratcliff and Smith, 2004; Bogacz et al., 2006) and participant groups (White et al., 2010; Starns and Ratcliff, 2012). However, the intuitions provided by the models about neural mechanisms that have guided recent neuroimaging studies (Forstmann et al., 2008, 2010; Mansfield et al., 2011; van Maanen et al., 2011) are inconsistent with neurophysiological mechanisms.

The diversity of results can be unified by recognizing that decision making is not a unitary process; "decide that" (categorization) and "decide to" (response selection) are semantically, logically, and mechanistically distinct (Schall, 2001). Visual neurons in LIP, FEF, and SC arrive at a representation of stimulus

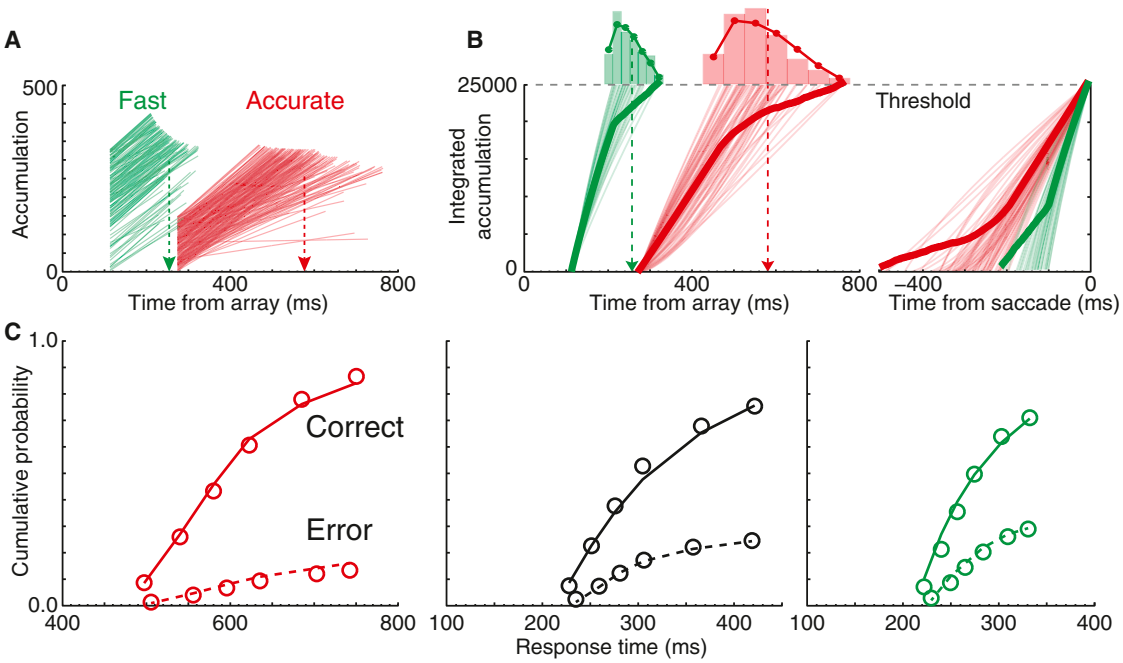

Figure 6. Integrated Accumulator Model

(A) Sample accumulation functions for correct trials from the best-fitting model for Fast and Accurate trials. Starting levels and slopes were highest for Fast, intermediate for Neutral (data not shown), and lowest for Accurate. Arrows denote mean simulated RT.

(B) Sample and average integrated accumulation functions aligned on array (left) and response (right). The distribution of finish times to an invariant threshold (histogram) reproduce distribution of RTs (overlaid).

(C) iA model predicts probability and times of correct and error responses across Accurate (left), Neutral (middle), and Fast (right) SAT conditions. Observed (circles) and predicted (lines) defective cumulative probability of correct (solid) and error (dashed) RTs are shown.

evidence categorizing targets and nontargets. This representation can be used to initiate a gradual response selection and preparation process that is completed when a ballistic motor phase is initiated that produces muscle contraction. This general hypothesis has been formalized in a model in which a search salience representation provides evidence that is accumulated by movement neurons to initiate a response (Purcell et al., 2010, 2012). This model utilizes gating inhibition to establish a criterion level of evidence representation necessary to begin response accumulation. It was demonstrated that SAT could be accomplished by elevating this gate to delay RT (Purcell et al., 2012). Our findings of the modulation of the salience representation in visual neurons and the direction of modulation of movement neuron activity were not anticipated by this or any other stochastic accumulator model.

Integrated Accumulator Model

The iA model reconciles the stochastic accumulator model framework with the neural data. The model is inspired by the insight that characteristics of postdecision motor processes constrain the stochastic decision accumulation process and is anchored on invariance at the beginning of the ballistic motor process. Variation in saccade velocity arises from variation in the magnitude of presaccadic movement activity (van Opstal and Goossens, 2008) and of OPN hyperpolarization (Yoshida et al., 1999). We found no variation of saccade velocity across the large variation of RT across SAT conditions. Hence, the magnitude of neural activity triggering the saccades must be invariant. The iA model achieves that invariance by integrating through time the evidence accumulator. We discovered that the slower accumulation to a lower terminal level in the Accurate condition integrated to the same value as the faster accumulation to a higher terminal level in the Fast condition. This leaky integration is regarded as a proxy for the net hyperpolarization of the OPNs that prevent saccade generation. The iA model architecture fit the performance measures as well as the typical LBA model while replicating key characteristics of the neural modulation. Recordings of SC and OPNs will be critical tests of this model.

The iA model is not proposed as a replacement for conventional accumulator models; it simply proves that the architecture embodied by the model is plausible. In fact, iA and LBA are mirrors of each other that emphasize different assumptions or aspects of the accumulation and response process. The mimicry of computational models with different architectures is well known (Dzhafarov, 1993; Ratcliff et al., 1999; Usher and McClelland, 2001; Ratcliff and Smith, 2004) and represents a fundamental problem of exclusively computational accounts (Moore, 1956).

The apparent incompatibility of stochastic accumulator models and the underlying neurophysiology exposes another important theoretical issue. Since Hanes and Schall (1996) first proposed that the activity of certain neurons can be identified with stochastic accumulator models, many investigators have

Table 2. Integrated Accumulator Parameter Estimates

Data Set	Baseline (A)	Integrated Threshold (b')	Drift Rate (v)	Nondecision Time (T_0)	Leak (τ)	Between-Trial Variability of Drift Rate (s)
Accurate	149	25,406	0.74	273	115	0.27
Neutral	290	25,406	0.83	99	115	0.27
Fast	328	25,406	0.92	112	115	0.27

Best-fitting parameter estimates for iA model with A, v, and T_0 free to vary across conditions and b and τ shared. Parameter s was fixed. Units for A, b', arbitrary units of activation; v, s, activation/ms; T_0, τ ms.

explored this in multiple brain regions (e.g., Roitman and Shadlen, 2002; Ratcliff et al., 2003, 2007; Ding and Gold, 2010, 2012). The unexpected diversity of effects observed with the SAT manipulation revealed that the mapping is not as simple as was imagined.

Limitations

The interpretation of this study rests on the following two major assumptions: (1) monkeys' performance of SAT is a useful model of human performance and (2) FEF neurons contribute essentially to the processes required for this task and SAT adjustments. We discuss each in turn.

The paradigm is comparable to that used in human SAT studies. With verbal instructions, humans have no difficulty producing deliberate, slow responses (Wickelgren, 1977). Monkeys prefer fast responding and are impervious to verbal instruction, so it was necessary to introduce temporal deadlines to train the monkeys. The following observations confirm that these data correspond usefully to human SAT performance. First, both monkeys sustained SAT performance when the deadline contingency was removed. Second, the patterns of neural modulation persisted when RT was equated across premature Accurate and late Fast responses or across Accurate and Fast trials subsampled to match median RT in Neutral trials. Indeed, our major conclusions would remain if we disregarded the Accurate condition altogether and compared the Neutral and Fast conditions alone. Finally, the range of correct and error RTs and percent correct were fit as well by the LBA as comparable data from humans (e.g., Forstmann et al., 2008). Thus, the conclusions cannot be rejected on the grounds that monkey SAT differs meaningfully from human SAT.

Second, perhaps FEF is not mediating the stochastic accumulation that accomplishes SAT. This possibility entails at least three logical possibilities: (1) FEF neural activity precedes the actual accumulation process, or (2) FEF neural activity follows the accumulation process. Both of these possibilities seem difficult to reconcile with the fact that the activity in FEF coincides with the interval during which a stochastic accumulator must be occurring to produce the response. (3) FEF has nothing at all to do with the accumulation process. This conclusion is difficult to reconcile with the aforementioned evidence obtained from multiple, independent empirical and modeling studies. Nevertheless, entertaining this notion, if the stochastic accumulation process is not in FEF, then where? One possibility is the SC, like FEF, receives inputs from multiple cortical visual areas (Lui et al., 1995; Schall et al., 1995) and projects to the brainstem saccade generator (Harting, 1977; Figure S5A). The target selection process during visual search occurs in SC (McPeek and Keller, 2002; Shen and Paré, 2007; Kim and Basso, 2008; White and Munoz, 2011), and the activity of presaccadic movement neurons in SC has been identified with stochastic accumulator models (Boucher et al., 2007; Ratcliff et al., 2007). However, given the dense network connectivity of SC and FEF and the equivalence of neural modulation during visual search and other tasks, it is difficult to understand how SC could be the bridge locus while FEF is not. Another possible bridge locus is posterior parietal cortex in which the activity of select neurons can be identified with evidence accumulation in a motion discrimination task (Gold and Shadlen, 2007). However, when tested in the motion discrimination task, neurons in FEF satisfy the same criteria, with the clearest examples being the movement neurons (Ding and Gold, 2012). Furthermore, during visual search, the activity of parietal neurons parallels that of the visual neurons in FEF (Gottlieb et al., 1998; Constantinidis and Steinmetz, 2005; Ipata et al., 2006; Buschman and Miller, 2007; Thomas and Paré, 2007; Balan et al., 2008; Ogawa and Komatsu, 2009), but parietal cortex has very few movement neurons (Gottlieb and Goldberg, 1999) and no direct projections to the brainstem saccade generator (May and Andersen, 1986; Schmahmann and Pandya, 1989). Thus, parietal cortex can contribute only indirectly to response production.

Conclusions

SAT occurs commonly and plays a key role in models of decision making. This work establishes a nonhuman primate model of the SAT and so opens the door to further study its neural mechanisms. Single-unit recordings revealed widespread and unexpected influence of SAT that cannot be readily accommodated by current models of the decision process. An integrated accumulator model reconciles the patterns of neural modulation with the stochastic accumulator framework. Neurophysiological data from other cortical and subcortical structures will be critical in establishing the generalizability of these results.

EXPERIMENTAL PROCEDURES

Task

Monkeys performed T/L visual search for a target item presented among seven distractor items. Trials began when monkeys fixated a central point for ~1,000 ms. Each monkey was extensively trained to associate the color of the fixation point (red, white, or green) with a SAT condition. After fixating, an isoeccentric array of T and L shapes appeared, of which one was the target item for that day. Distractor items were drawn randomly from the nontarget set and oriented randomly in the cardinal positions. For a few sessions, all distractor items were oriented identically, but this had no effect on behavioral or neural data.

Trials were run in blocks of 10–20 trials. In the Accurate condition, saccades to the target item were rewarded if RT exceeded an unsignaled deadline. Pilot

testing of each monkey led to a deadline at which ~20% of responses were too fast (Q: 500 ms; S: 425 ms). Errant saccades and saccades that were correct but too fast were followed by a 4,000 ms time out. In the Neutral condition, saccades to the target item with any RT were rewarded. Errant saccades were met with a 2,000 ms time out. In the Fast condition, correct saccades were rewarded if RT preceded a deadline such that ~20% of responses were too slow (Q: 365 ms; S: 385 ms). RTs exceeding the deadline (whether or not accurate) were followed by a 4,000 ms time out. Inaccurate saccades within the deadline had no time out. However, monkeys had difficulty discriminating lack of reward from an inaccurate saccade and lack of reward from slow responding. Hence, the display was removed on 25%–50% of missed-deadline trials. Monkeys quickly learned that reinforcement was only available prior to this time. All patterns of results and conclusions were unchanged by these trials. Monkeys respected the response deadlines (proportion of missed deadlines: Q Accurate: 0.18, Fast: 0.16; S Accurate: 0.19, Fast: 0.13). Some sessions included only the Fast and Accurate conditions; for that reason, variability should be expected to be higher in the Neutral condition.

Neurophysiology

We recorded neurons in FEF, located on the anterior bank of the arcuate sulcus, using tungsten microelectrodes (2–4 MΩ, FHC) referenced to a guide tube in contact with the dura. Location was verified by evoking eye movements though low-threshold (<50 μA) microstimulation. The number of electrodes lowered on a given session ranged from one to eight. Single-unit waveforms were isolated online, sampled at 40 kHz, and resorted offline (Offline Sorter; Plexon). All surgical and experimental procedures were in accordance with the National Institutes of Health Guide for the Care and Use of Laboratory Animals and approved by the Vanderbilt Institutional Animal Care and Use Committee.

Neuron Types

Neurons are categorized into three major types: visual, visuomovement, and movement. Though classification operates along a continuum, many observations demonstrate that these populations are functionally distinct (Cohen et al., 2009; Ray et al., 2009; Gregoriou et al., 2012). Visual neurons increase discharge rates significantly immediately after array presentation but have no saccade-related modulation. Movement neurons increase discharge rate significantly before saccade initiation but have no visual response. Visuomovement neurons exhibit both periods of modulation. To classify neurons, we used activity from a memory-guided saccade task. To test for visual responses, we used t tests to compare the average activity in the interval 75–100 ms after target presentation to the activity in the 100 ms interval preceding target presentation. To test for presaccadic activity, we used t tests to compare the average activity in the 100 ms interval before saccade initiation to the activity in the interval 500–400 ms before saccade initiation.

Proactive Modulation and Target Selection Time

To determine when neurons responded differently to two SAT conditions or when the target as compared to distractors appeared in the RF, we computed ms-by-ms Wilcoxon rank-sum tests, evaluating the null hypothesis that target-in-RF activity was significantly different from distractor-in-RF activity. Target selection time (TST) was the first of ten successive time points significant at the $p < 0.01$ level. Population TST was computed using jackknifing.

Statistical Analyses

Spike trains were convolved with a kernel that resembled a postsynaptic potential to create a spike density function (SDF). For population analyses, SDFs were normalized to the peak average activity irrespective of all conditions and behavioral outcome (i.e., over all SAT conditions, all RT, correct and errant responses, etc.) in a particular session. Because not all sessions included the Neutral condition, we had to deal with the problem of missing data. To respect the fact that these data were paired observations while obviating the need to drop missing cases, we took a regression-based approach (Lorch and Myers, 1990). Succinctly, we estimated the slope of a regression line considering average neural activity patterns in the Accurate, Neutral, and Fast conditions when all were available; when only the Accurate and Fast conditions were available, the slope was estimated using only those two conditions. This was computed separately for each individual neuron, and the resulting parameter estimates were tested against 0 using a one-sample t test.

Accumulator Model

We fit behavioral data with the LBA (Brown and Heathcote, 2008). Although simpler than stochastic accumulator models, it has been used in several recent studies of SAT (Forstmann et al., 2008, 2010; Mansfield et al., 2011; van Maanen et al., 2011; Ho et al., 2012), and conclusions derived from any of these models agree (Donkin et al., 2011b). LBA includes the following five parameters: A (maxima of start point distribution), b (threshold), v (drift rate), T_0 (nondecision time), and s (between-trial variability in drift rate; Figure 1E, inset). As is common, s was fixed to 0.10 for all models, leaving four parameters (A, b, v, and T_0) that were shared or free to vary across SAT conditions. To reduce model complexity, we assumed equivalence between all nontarget units, leading to a race between two accumulators: one representing the target stimulus and one representing distractor items. The drift rate for distractor items was set to $1 - v$. Outliers (median ± 1.5 × the interquartile range, calculated separately for each SAT condition) were removed. We fit 16 variants, representing all possible combinations of free and shared parameters, using established methodology (Donkin et al., 2009, 2011a). Models were fit to the observed defective CDFs that were normalized to mean accuracy rate (Ratcliff and Tuerlinckx, 2002), using maximum likelihood estimation. Fits obtained for single sessions and across the population led to identical conclusions: the threshold parameter (b) was the most critical in accounting for SAT-related variability.

Leaky Integration of Movement Neuron Activity

We submitted the FEF movement activity to a leaky integrator according to

$$i(t) = dt[I(t) + A(t) - i(t)/\tau]$$

where i is the value of the integrator at time $t > 0$, A is the value of neural activity at time $t > 0$, and τ is a decay constant varied from 1 to 1,000 ms. Each integrator was initialized to 0 at the beginning of each trial. Time step dt was set to 1 ms. We computed the leaky integration for each neuron, with movement activity integrated trial-by-trial from search array presentation until saccade initiation. For each condition and decay, the value of the integral 20–10 ms before saccade initiation was recorded as the trigger threshold (Figure S5B). We found that the trigger threshold was invariant with respect to task conditions (Fast/Neutral/Accurate condition) and made or missed deadline (premature Accurate/late Fast) when the decay constant was in the range of plausible values ($7.1 \text{ ms} < \tau < 166.7$; McCormick et al., 1985). What differed between SAT conditions was the amount of time needed for this integration to reach a single, constant threshold (Figures 5 and S5B). We also computed the time course of integration for each RT quantile, separated by made/missed deadline and SAT condition. Remarkably, the trigger thresholds remained constant for both movement and visuomovement neurons (Figures S5B and S5C).

Integrated Accumulator Model

For each of 5,000 simulated trials per SAT condition, a start point (A) was drawn from a uniform distribution, and a drift rate (v) was drawn from a normal distribution with standard deviation s. The drift rate for distractor items was set to $1 - v$. Activation functions that increased linearly with rate v were integrated with leak τ in the same manner as the movement activity described above. The values for A, v, and nondecision time T_0 were allowed to vary between SAT conditions. Leakage τ was not fixed but was shared across SAT conditions because cognitive state is unlikely to influence brainstem saccade-triggering mechanisms. The distribution of simulated RTs and proportions correct were compared against Vincentized behavioral data using χ^2. Outliers were removed from the behavioral and simulated data by eliminating values beyond median ± 1.5 × the interquartile range for each condition separately. Data are presented as defective CDFs, normalized to the mean accuracy rate. Minimization was carried out in several steps, first using multiple runs of the genetic algorithm in MATLAB with different random number seeds and values for s. The best fitting of these were minimized again with bounded simplex algorithms.

SUPPLEMENTAL INFORMATION

Supplemental Information includes five figures and one movie and can be found with this article online at http://dx.doi.org/10.1016/j.neuron.2012.08.030.

ACKNOWLEDGMENTS

This work was supported by F32-EY019851 to R.P.H. and by R01-EY08890, P30-EY08126, P30-HD015052, and the E. Bronson Ingram Chair in Neuroscience. We would like to thank S. Brown, J. Cohen, R. Desimone, P. Holmes, G. Logan, A. Maier, P. Middlebrooks, T. Palmeri, M. Paré, B. Purcell, R. Ramachandran, R. Ratcliff, F. Tong, M. Wallace, X.J. Wang, and B. Zandbelt for comments. R.P.H. designed the study, collected the data, and analyzed the results. R.P.H. and J.D.S. wrote the paper.

Accepted: August 16, 2012
Published: November 7, 2012

REFERENCES

Balan, P.F., Oristaglio, J., Schneider, D.M., and Gottlieb, J. (2008). Neuronal correlates of the set-size effect in monkey lateral intraparietal area. PLoS Biol. *6*, e158.

Basso, M.A., and Wurtz, R.H. (2002). Neuronal activity in substantia nigra pars reticulata during target selection. J. Neurosci. *22*, 1883–1894.

Bogacz, R., Brown, E., Moehlis, J., Holmes, P., and Cohen, J.D. (2006). The physics of optimal decision making: a formal analysis of models of performance in two-alternative forced-choice tasks. Psychol. Rev. *113*, 700–765.

Bogacz, R., Wagenmakers, E.-J., Forstmann, B.U., and Nieuwenhuis, S. (2010). The neural basis of the speed-accuracy tradeoff. Trends Neurosci. *33*, 10–16.

Boucher, L., Palmeri, T.J., Logan, G.D., and Schall, J.D. (2007). Inhibitory control in mind and brain: an interactive race model of countermanding saccades. Psychol. Rev. *114*, 376–397.

Brown, S.D., and Heathcote, A. (2008). The simplest complete model of choice response time: linear ballistic accumulation. Cognit. Psychol. *57*, 153–178.

Bruce, C.J., and Goldberg, M.E. (1985). Primate frontal eye fields. I. Single neurons discharging before saccades. J. Neurophysiol. *53*, 603–635.

Buschman, T.J., and Miller, E.K. (2007). Top-down versus bottom-up control of attention in the prefrontal and posterior parietal cortices. Science *315*, 1860–1862.

Büttner-Ennever, J.A., Cohen, B., Pause, M., and Fries, W. (1988). Raphe nucleus of the pons containing omnipause neurons of the oculomotor system in the monkey, and its homologue in man. J. Comp. Neurol. *267*, 307–321.

Chittka, L., Dyer, A.G., Bock, F., and Dornhaus, A. (2003). Psychophysics: bees trade off foraging speed for accuracy. Nature *424*, 388.

Cisek, P., Puskas, G.A., and El-Murr, S. (2009). Decisions in changing conditions: the urgency-gating model. J. Neurosci. *29*, 11560–11571.

Cohen, J.Y., Pouget, P., Heitz, R.P., Woodman, G.F., and Schall, J.D. (2009). Biophysical support for functionally distinct cell types in the frontal eye field. J. Neurophysiol. *101*, 912–916.

Constantinidis, C., and Steinmetz, M.A. (2005). Posterior parietal cortex automatically encodes the location of salient stimuli. J. Neurosci. *25*, 233–238.

Ding, L., and Gold, J.I. (2010). Caudate encodes multiple computations for perceptual decisions. J. Neurosci. *30*, 15747–15759.

Ding, L., and Gold, J.I. (2012). Neural correlates of perceptual decision making before, during, and after decision commitment in monkey frontal eye field. Cereb. Cortex *22*, 1052–1067.

Donkin, C., Averell, L., Brown, S., and Heathcote, A. (2009). Getting more from accuracy and response time data: methods for fitting the linear ballistic accumulator. Behav. Res. Methods *41*, 1095–1110.

Donkin, C., Brown, S., and Heathcote, A. (2011a). Drawing conclusions from choice response time models: A tutorial using the linear ballistic accumulator. J. Math. Psychol. *55*, 140–151.

Donkin, C., Brown, S., Heathcote, A., and Wagenmakers, E.-J. (2011b). Diffusion versus linear ballistic accumulation: different models but the same conclusions about psychological processes? Psychon. Bull. Rev. *18*, 61–69.

Dzhafarov, E.N. (1993). Grice-representability of response time distribution families. Psychometrika *58*, 281–314.

Everling, S., and Munoz, D.P. (2000). Neuronal correlates for preparatory set associated with pro-saccades and anti-saccades in the primate frontal eye field. J. Neurosci. *20*, 387–400.

Everling, S., Dorris, M.C., Klein, R.M., and Munoz, D.P. (1999). Role of primate superior colliculus in preparation and execution of anti-saccades and pro-saccades. J. Neurosci. *19*, 2740–2754.

Fitts, P.M. (1966). Cognitive aspects of information processing. 3. Set for speed versus accuracy. J. Exp. Psychol. *71*, 849–857.

Forstmann, B.U., Dutilh, G., Brown, S., Neumann, J., von Cramon, D.Y., Ridderinkhof, K.R., and Wagenmakers, E.J. (2008). Striatum and pre-SMA facilitate decision-making under time pressure. Proc. Natl. Acad. Sci. USA *105*, 17538–17542.

Forstmann, B.U., Anwander, A., Schäfer, A., Neumann, J., Brown, S., Wagenmakers, E.-J., Bogacz, R., and Turner, R. (2010). Cortico-striatal connections predict control over speed and accuracy in perceptual decision making. Proc. Natl. Acad. Sci. USA *107*, 15916–15920.

Gold, J.I., and Shadlen, M.N. (2007). The neural basis of decision making. Annu. Rev. Neurosci. *30*, 535–574.

Gottlieb, J., and Goldberg, M.E. (1999). Activity of neurons in the lateral intraparietal area of the monkey during an antisaccade task. Nat. Neurosci. *2*, 906–912.

Gottlieb, J.P., Kusunoki, M., and Goldberg, M.E. (1998). The representation of visual salience in monkey parietal cortex. Nature *391*, 481–484.

Gregoriou, G.G., Gotts, S.J., and Desimone, R. (2012). Cell-type-specific synchronization of neural activity in FEF with V4 during attention. Neuron *73*, 581–594.

Hanes, D.P., and Schall, J.D. (1996). Neural control of voluntary movement initiation. Science *274*, 427–430.

Harting, J.K. (1977). Descending pathways from the superior collicullus: an autoradiographic analysis in the rhesus monkey (Macaca mulatta). J. Comp. Neurol. *173*, 583–612.

Heitz, R.P., and Engle, R.W. (2007). Focusing the spotlight: individual differences in visual attention control. J. Exp. Psychol. Gen. *136*, 217–240.

Heitz, R.P., Cohen, J.Y., Woodman, G.F., and Schall, J.D. (2010). Neural correlates of correct and errant attentional selection revealed through N2pc and frontal eye field activity. J. Neurophysiol. *104*, 2433–2441.

Ho, T., Brown, S., van Maanen, L., Forstmann, B.U., Wagenmakers, E.J., and Serences, J.T. (2012). The optimality of sensory processing during the speed-accuracy tradeoff. J. Neurosci. *32*, 7992–8003.

Huerta, M.F., Krubitzer, L.A., and Kaas, J.H. (1986). Frontal eye field as defined by intracortical microstimulation in squirrel monkeys, owl monkeys, and macaque monkeys: I. Subcortical connections. J. Comp. Neurol. *253*, 415–439.

Ipata, A.E., Gee, A.L., Goldberg, M.E., and Bisley, J.W. (2006). Activity in the lateral intraparietal area predicts the goal and latency of saccades in a free-viewing visual search task. J. Neurosci. *26*, 3656–3661.

Ivanoff, J., Branning, P., and Marois, R. (2008). fMRI evidence for a dual process account of the speed-accuracy tradeoff in decision-making. PLoS ONE *3*, e2635.

Kanda, T., Iwamoto, Y., Yoshida, K., and Shimazu, H. (2007). Glycinergic inputs cause the pause of pontine omnipause neurons during saccades. Neurosci. Lett. *413*, 16–20.

Kaneko, H., Tamura, H., Kawashima, T., and Suzuki, S.S. (2006). A choice reaction-time task in the rat: a new model using air-puff stimuli and lever-release responses. Behav. Brain Res. *174*, 151–159.

Kim, B., and Basso, M.A. (2008). Saccade target selection in the superior colliculus: a signal detection theory approach. J. Neurosci. *28*, 2991–3007.

Langer, T.P., and Kaneko, C.R. (1990). Brainstem afferents to the oculomotor omnipause neurons in monkey. J. Comp. Neurol. *295*, 413–427.

Lee, K.-M., and Keller, E.L. (2008). Neural activity in the frontal eye fields modulated by the number of alternatives in target choice. J. Neurosci. *28*, 2242–2251.

Lorch, R.F., Jr., and Myers, J.L. (1990). Regression analyses of repeated measures data in cognitive research. J. Exp. Psychol. Learn. Mem. Cogn. *16*, 149–157.

Lui, F., Gregory, K.M., Blanks, R.H., and Giolli, R.A. (1995). Projections from visual areas of the cerebral cortex to pretectal nuclear complex, terminal accessory optic nuclei, and superior colliculus in macaque monkey. J. Comp. Neurol. *363*, 439–460.

Mansfield, E.L., Karayanidis, F., Jamadar, S., Heathcote, A., and Forstmann, B.U. (2011). Adjustments of response threshold during task switching: a model-based functional magnetic resonance imaging study. J. Neurosci. *31*, 14688–14692.

May, J.G., and Andersen, R.A. (1986). Different patterns of corticopontine projections from separate cortical fields within the inferior parietal lobule and dorsal prelunate gyrus of the macaque. Exp. Brain Res. *63*, 265–278.

McCormick, D.A., Connors, B.W., Lighthall, J.W., and Prince, D.A. (1985). Comparative electrophysiology of pyramidal and sparsely spiny stellate neurons of the neocortex. J. Neurophysiol. *54*, 782–806.

McPeek, R.M., and Keller, E.L. (2002). Saccade target selection in the superior colliculus during a visual search task. J. Neurophysiol. *88*, 2019–2034.

Miller, J. (1983). Can response preparation begin before stimulus recognition finishes? J. Exp. Psychol. Hum. Percept. Perform. *9*, 161–182.

Moore, E.F. (1956). Gedanken-Experiments on sequential machines. In Automata Studies, C.E. Shannon and J. McCarthy, eds. (Princeton, NJ: Princeton University Press), pp. 129–153.

Murthy, A., Ray, S., Shorter, S.M., Schall, J.D., and Thompson, K.G. (2009). Neural control of visual search by frontal eye field: effects of unexpected target displacement on visual selection and saccade preparation. J. Neurophysiol. *101*, 2485–2506.

Ogawa, T., and Komatsu, H. (2006). Neuronal dynamics of bottom-up and top-down processes in area V4 of macaque monkeys performing a visual search. Exp. Brain Res. *173*, 1–13.

Ogawa, T., and Komatsu, H. (2009). Condition-dependent and condition-independent target selection in the macaque posterior parietal cortex. J. Neurophysiol. *101*, 721–736.

Osman, A., Moore, C.M., and Ulrich, R. (1995). Bisecting RT with lateralized readiness potentials: precue effects of LRP onset. Acta Psychol. (Amst.) *90*, 111–127.

Osman, A., Lou, L., Müller-Gethmann, H., Rinkenauer, G., Mattes, S., and Ulrich, R. (2000). Mechanisms of speed-accuracy tradeoff: evidence from covert motor processes. Biol. Psychol. *51*, 173–199.

Paré, M., and Hanes, D.P. (2003). Controlled movement processing: superior colliculus activity associated with countermanded saccades. J. Neurosci. *23*, 6480–6489.

Purcell, B.A., Heitz, R.P., Cohen, J.Y., Schall, J.D., Logan, G.D., and Palmeri, T.J. (2010). Neurally constrained modeling of perceptual decision making. Psychol. Rev. *117*, 1113–1143.

Purcell, B.A., Schall, J.D., Logan, G.D., and Palmeri, T.J. (2012). From salience to saccades: multiple-alternative gated stochastic accumulator model of visual search. J. Neurosci. *32*, 3433–3446.

Ratcliff, R., and Smith, P.L. (2004). A comparison of sequential sampling models for two-choice reaction time. Psychol. Rev. *111*, 333–367.

Ratcliff, R., and Tuerlinckx, F. (2002). Estimating parameters of the diffusion model: approaches to dealing with contaminant reaction times and parameter variability. Psychon. Bull. Rev. *9*, 438–481.

Ratcliff, R., Van Zandt, T., and McKoon, G. (1999). Connectionist and diffusion models of reaction time. Psychol. Rev. *106*, 261–300.

Ratcliff, R., Cherian, A., and Segraves, M. (2003). A comparison of macaque behavior and superior colliculus neuronal activity to predictions from models of two-choice decisions. J. Neurophysiol. *90*, 1392–1407.

Ratcliff, R., Hasegawa, Y.T., Hasegawa, R.P., Smith, P.L., and Segraves, M.A. (2007). Dual diffusion model for single-cell recording data from the superior colliculus in a brightness-discrimination task. J. Neurophysiol. *97*, 1756–1774.

Ray, S., Pouget, P., and Schall, J.D. (2009). Functional distinction between visuomovement and movement neurons in macaque frontal eye field during saccade countermanding. J. Neurophysiol. *102*, 3091–3100.

Raybourn, M.S., and Keller, E.L. (1977). Colliculoreticular organization in primate oculomotor system. J. Neurophysiol. *40*, 861–878.

Requin, J., and Riehle, A. (1995). Neural correlates of partial transmission of sensorimotor information in the cerebral cortex. Acta Psychol. (Amst.) *90*, 81–95.

Rinkenauer, G., Osman, A., Ulrich, R., Muller-Gethmann, H., and Mattes, S. (2004). On the locus of speed-accuracy trade-off in reaction time: inferences from the lateralized readiness potential. J. Exp. Psychol. Gen. *133*, 261–282.

Roitman, J.D., and Shadlen, M.N. (2002). Response of neurons in the lateral intraparietal area during a combined visual discrimination reaction time task. J. Neurosci. *22*, 9475–9489.

Sato, T.R., and Schall, J.D. (2003). Effects of stimulus-response compatibility on neural selection in frontal eye field. Neuron *38*, 637–648.

Sato, T., Murthy, A., Thompson, K.G., and Schall, J.D. (2001). Search efficiency but not response interference affects visual selection in frontal eye field. Neuron *30*, 583–591.

Scangos, K.W., and Stuphorn, V. (2010). Medial frontal cortex motivates but does not control movement initiation in the countermanding task. J. Neurosci. *30*, 1968–1982.

Schafer, R.J., and Moore, T. (2011). Selective attention from voluntary control of neurons in prefrontal cortex. Science *332*, 1568–1571.

Schall, J.D. (1991). Neuronal activity related to visually guided saccades in the frontal eye fields of rhesus monkeys: comparison with supplementary eye fields. J. Neurophysiol. *66*, 559–579.

Schall, J.D. (2001). Neural basis of deciding, choosing and acting. Nat. Rev. Neurosci. *2*, 33–42.

Schall, J.D., Morel, A., King, D.J., and Bullier, J. (1995). Topography of visual cortex connections with frontal eye field in macaque: convergence and segregation of processing streams. J. Neurosci. *15*, 4464–4487.

Schmahmann, J.D., and Pandya, D.N. (1989). Anatomical investigation of projections to the basis pontis from posterior parietal association cortices in rhesus monkey. J. Comp. Neurol. *289*, 53–73.

Scudder, C.A., Kaneko, C.S., and Fuchs, A.F. (2002). The brainstem burst generator for saccadic eye movements: a modern synthesis. Exp. Brain Res. *142*, 439–462.

Segraves, M.A. (1992). Activity of monkey frontal eye field neurons projecting to oculomotor regions of the pons. J. Neurophysiol. *68*, 1967–1985.

Shen, K., and Paré, M. (2007). Neuronal activity in superior colliculus signals both stimulus identity and saccade goals during visual conjunction search. J. Vis. *7*, 15, 1–13.

Shinoda, Y., Sugiuchi, Y., Izawa, Y., and Takahashi, M. (2008). Neural circuits for triggering saccades in the brainstem. Prog. Brain Res. *171*, 79–85.

Standage, D., You, H., Wang, D.-H., and Dorris, M.C. (2011). Gain modulation by an urgency signal controls the speed-accuracy trade-off in a network model of a cortical decision circuit. Front Comput Neurosci *5*, 7.

Stanton, G.B., Goldberg, M.E., and Bruce, C.J. (1988). Frontal eye field efferents in the macaque monkey: II. Topography of terminal fields in midbrain and pons. J. Comp. Neurol. *271*, 493–506.

Starns, J.J., and Ratcliff, R. (2012). Age-related differences in diffusion model boundary optimality with both trial-limited and time-limited tasks. Psychon. Bull. Rev. *19*, 139–145.

Sternberg, S. (2001). Separate modifiability, mental modules, and the use of pure and composite measures to reveal them. Acta Psychol. (Amst.) *106*, 147–246.

Stroeymeyt, N., Giurfa, M., and Franks, N.R. (2010). Improving decision speed, accuracy and group cohesion through early information gathering in house-hunting ants. PLoS ONE *5*, 5.

Stuphorn, V., and Schall, J.D. (2006). Executive control of countermanding saccades by the supplementary eye field. Nat. Neurosci. *9*, 925–931.

Stuphorn, V., Brown, J.W., and Schall, J.D. (2010). Role of supplementary eye field in saccade initiation: executive, not direct, control. J. Neurophysiol. *103*, 801–816.

Thomas, N.W.D., and Paré, M. (2007). Temporal processing of saccade targets in parietal cortex area LIP during visual search. J. Neurophysiol. *97*, 942–947.

Thompson, K.G., Hanes, D.P., Bichot, N.P., and Schall, J.D. (1996). Perceptual and motor processing stages identified in the activity of macaque frontal eye field neurons during visual search. J. Neurophysiol. *76*, 4040–4055.

Usher, M., and McClelland, J.L. (2001). The time course of perceptual choice: the leaky, competing accumulator model. Psychol. Rev. *108*, 550–592.

Van Horn, M.R., Mitchell, D.E., Massot, C., and Cullen, K.E. (2010). Local neural processing and the generation of dynamic motor commands within the saccadic premotor network. J. Neurosci. *30*, 10905–10917.

van Maanen, L., Brown, S.D., Eichele, T., Wagenmakers, E.J., Ho, T., Serences, J., and Forstmann, B.U. (2011). Neural correlates of trial-to-trial fluctuations in response caution. J. Neurosci. *31*, 17488–17495.

van Opstal, A.J., and Goossens, H.H.L.M. (2008). Linear ensemble-coding in midbrain superior colliculus specifies the saccade kinematics. Biol. Cybern. *98*, 561–577.

van Veen, V., Krug, M.K., and Carter, C.S. (2008). The neural and computational basis of controlled speed-accuracy tradeoff during task performance. J. Cogn. Neurosci. *20*, 1952–1965.

Wenzlaff, H., Bauer, M., Maess, B., and Heekeren, H.R. (2011). Neural characterization of the speed-accuracy tradeoff in a perceptual decision-making task. J. Neurosci. *31*, 1254–1266.

White, B.J., and Munoz, D.P. (2011). Separate visual signals for saccade initiation during target selection in the primate superior colliculus. J. Neurosci. *31*, 1570–1578.

White, C.N., Ratcliff, R., Vasey, M.W., and McKoon, G. (2010). Using diffusion models to understand clinical disorders. J. Math. Psychol. *54*, 39–52.

Wickelgren, W.A. (1977). Speed-accuracy tradeoff and information processing dynamics. Acta Psychol. (Amst.) *41*, 67–85.

Wong, K.-F., Huk, A.C., Shadlen, M.N., and Wang, X.-J. (2007). Neural circuit dynamics underlying accumulation of time-varying evidence during perceptual decision making. Front Comput. Neurosci. *1*, 6.

Woodman, G.F., Kang, M.-S., Thompson, K., and Schall, J.D. (2008). The effect of visual search efficiency on response preparation: neurophysiological evidence for discrete flow. Psychol. Sci. *19*, 128–136.

Wyder, M.T., Massoglia, D.P., and Stanford, T.R. (2004). Contextual modulation of central thalamic delay-period activity: representation of visual and saccadic goals. J. Neurophysiol. *91*, 2628–2648.

Yoshida, K., Iwamoto, Y., Chimoto, S., and Shimazu, H. (1999). Saccade-related inhibitory input to pontine omnipause neurons: an intracellular study in alert cats. J. Neurophysiol. *82*, 1198–1208.

Neuron, Volume *76*

Supplemental Information

Neural Mechanisms of Speed-Accuracy Tradeoff

Richard P. Heitz and Jeffrey D. Schall

SUPPLEMENTAL FIGURES AND LEGENDS

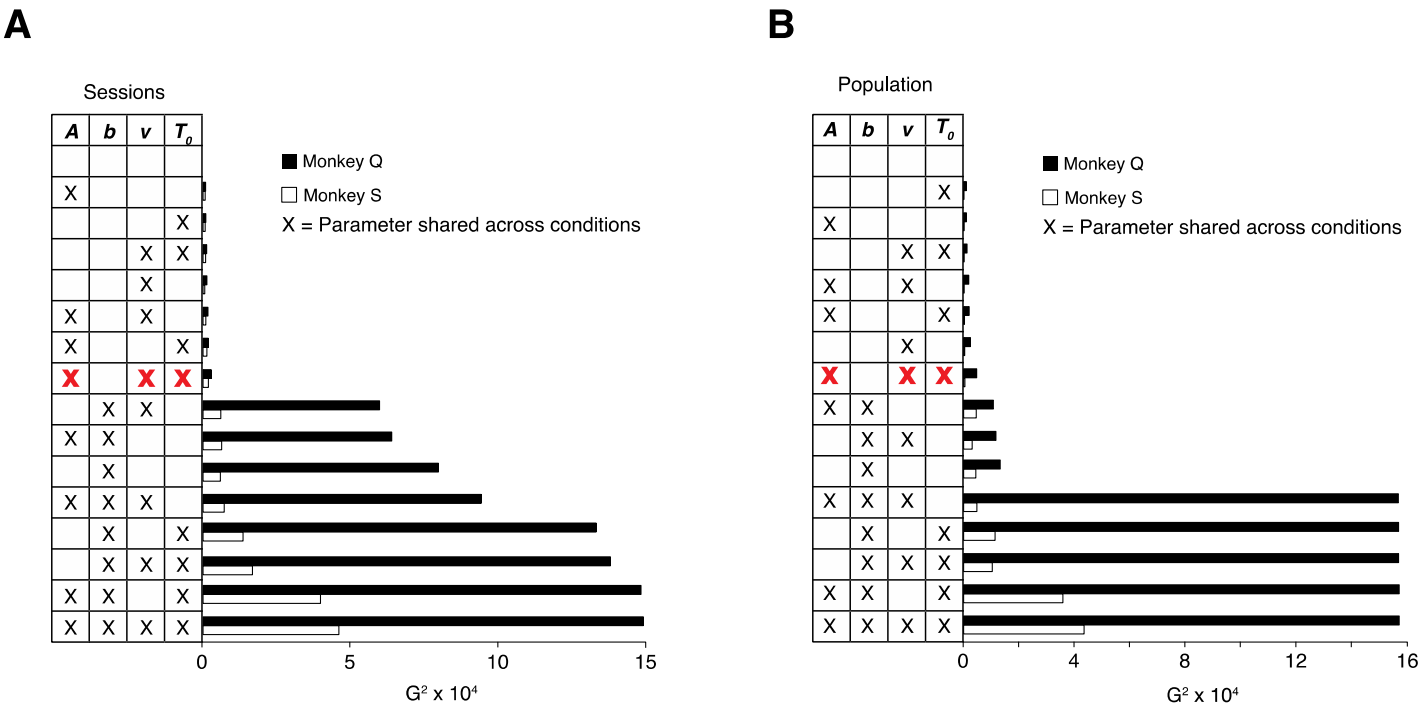

Figure S1. Fit statistics averaged across sessions (**A**) and averaged over all trials combined from all sessions (**B**). G^2 statistic was calculated as 2 x [LL_{full} – $LL_{restricted}$] where LL_{full} corresponds to the log likelihood from a model where all parameters were free to vary across conditions and $LL_{restricted}$ corresponds to log likelihood obtained from other models under consideration. Higher G^2 values indicate more deviation from the best-fitting, unrestricted model. G^2 values increase drastically when the threshold parameter (*b*) is fixed. Marked cells correspond to a fixed parameter, unmarked cells denote shared parameters. Fits from the model highlighted red are plotted in **Figure 1D-F**.

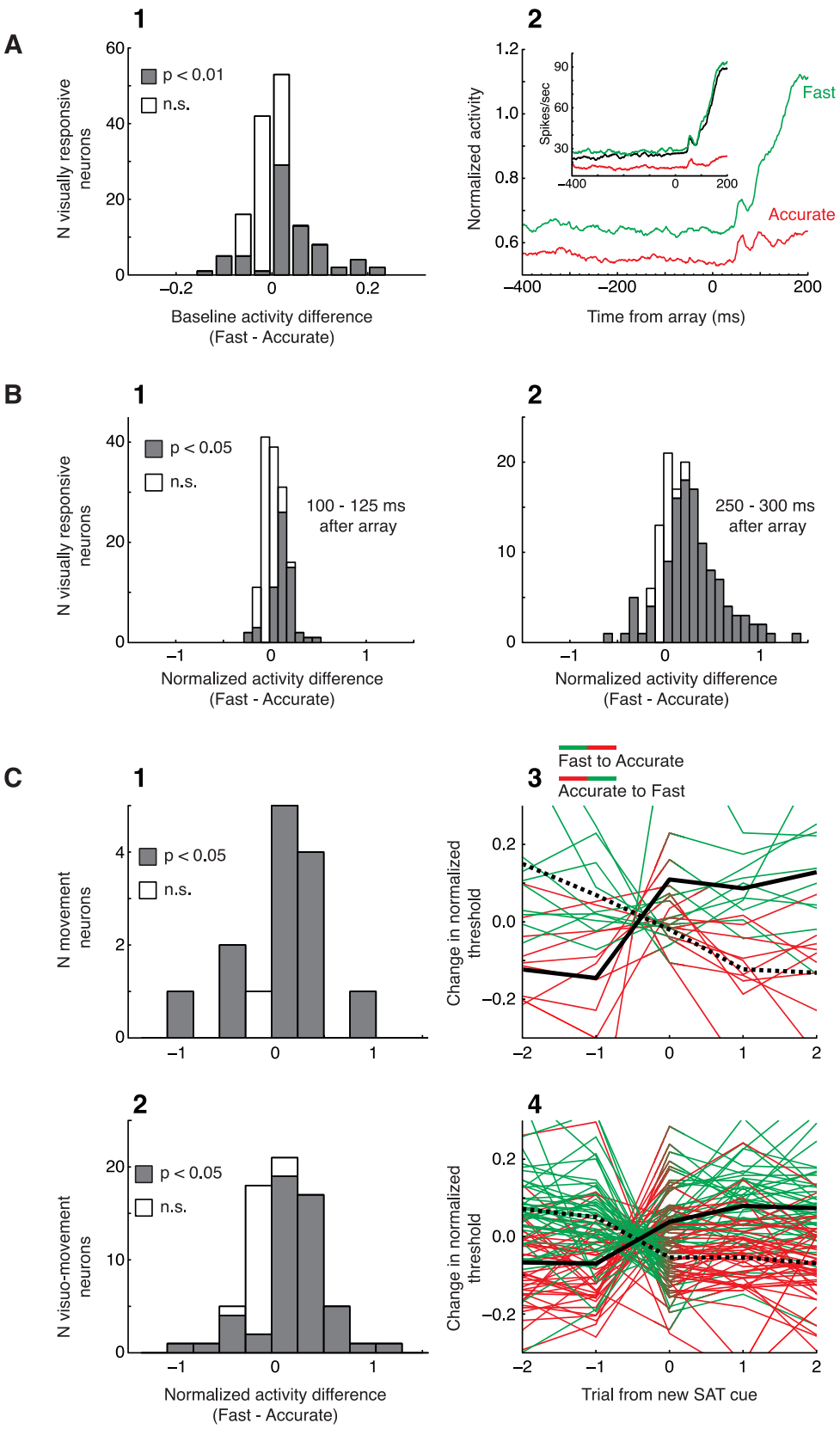

Figure S2. SAT-related neural modulation in FEF.
A, Baseline modulation. **A1**, The activity of 146 visually-responsive cells was averaged in the interval 300 ms before array presentation. All trials were included irrespective of trial type or behavioral outcome. Significant proactive modulation of baseline activity was observed in 54% of all visual and visuomovement neurons (two-tailed *t*-tests, all $p < 0.01$, filled bars). **A2,** The average activity in movement cells was tested in the interval 300 ms before array presentation. All trials were included irrespective of trial type or behavioral outcome. Significantly elevated baseline activity in the Fast relative to Accurate condition was observed in 29% of the 14 movement neurons recorded ($t_3 = -3.0$, $p = 0.06$). Only 1 of these neurons included data in the Neutral condition (inset).
B, Sensory gain modulation. The activity of 146 visually-responsive cells was averaged in the interval 100-125 ms (**B1**) and 250-300 ms (**B2**) after array presentation. Only correct Target-in-RF trials were included. Significantly elevated sensory gain in the Fast relative to Accurate condition was observed in 39% of neurons in the earlier period and 71% in the later period (two-tailed *t*-tests, all $p < 0.05$, filled bars).
C, Response threshold modulation. The activity of 14 movement (**C1, C3**) and 70 visuomovement (**C2, C4**) neurons was averaged in the interval 20-10 ms before saccade initiation. Only correct Target-in-RF trials were included. Significantly elevated response threshold in the Fast relative to Accurate condition was observed in the majority of movement neurons (71%) and visuomovement neurons (63%) (two-tailed *t*-tests, all $p < 0.05$, filled bars). The change in response threshold was immediate upon presentation of a new SAT cue (**C3**, movement neurons: Accurate to Fast: $t_{13} = -1.9$, $p = .08$; Fast to Accurate: $t_{13} = 2.6$, $p < 0.05$, two-tailed *t*-tests; **C4**, visuomovement neurons: Accurate to Fast: $t_{69} = -7.3$, Fast to Accurate: $t_{69} = 6.4$, all $p < 0.001$, two-tailed *t*-tests).

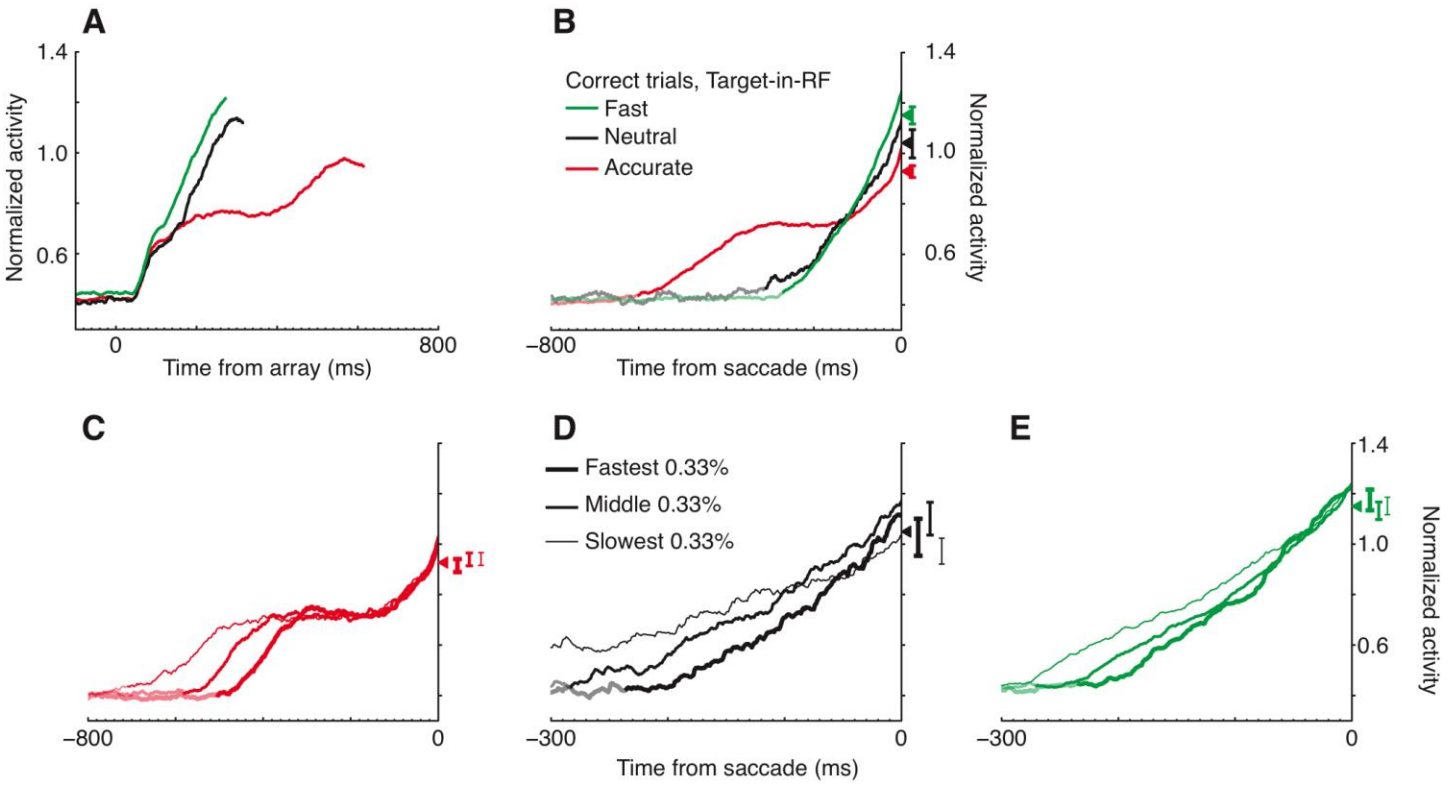

Figure S3. Adjustment of visuomovement neuron activity for SAT.
A, Average normalized discharge rate of all visuomovement neurons for correct trials when the target fell in the neuron's movement field, aligned on array presentation. Plots are truncated at mean RT. Note that the baseline adjustment reported in text is obscured by the averaging across neurons with and without the effect.
B, Average normalized discharge rate of all visuomovement neurons for correct trials when the target fell in the neuron's movement field, aligned on saccade initiation. Activity before mean RT is plotted lighter. On average, the slope of activity in the 100 ms preceding saccade increased with speed stress (Accurate: 2.1 < Neutral: 3.0 < Fast: 4.2 normalized sp/s^2; t_{69} = 4.5, p < 0.001, linear regression). Activity 20-10 ms before saccade increased with speed stress (t_{69} = 5.2, p < 0.001, linear regression). Note the appearance of a tonic level of activity in the Accurate condition. This is due solely to the temporal smearing of the visual onset response characteristic of visuomovement neurons. It is most evident in the Accurate condition due to the temporal separation between visual and movement response.
C-E, Discharge rates in Accurate, Neutral and Fast (bottom) conditions for correct Target-in-RF trials separated into fastest (thick), intermediate (thinner) and longest (thinnest) RT quantiles. Activity 20-10 ms before saccade varied across but not within SAT conditions (all p > 0.05, linear regression). All vertical bars represent $\pm$ 1 SEM.

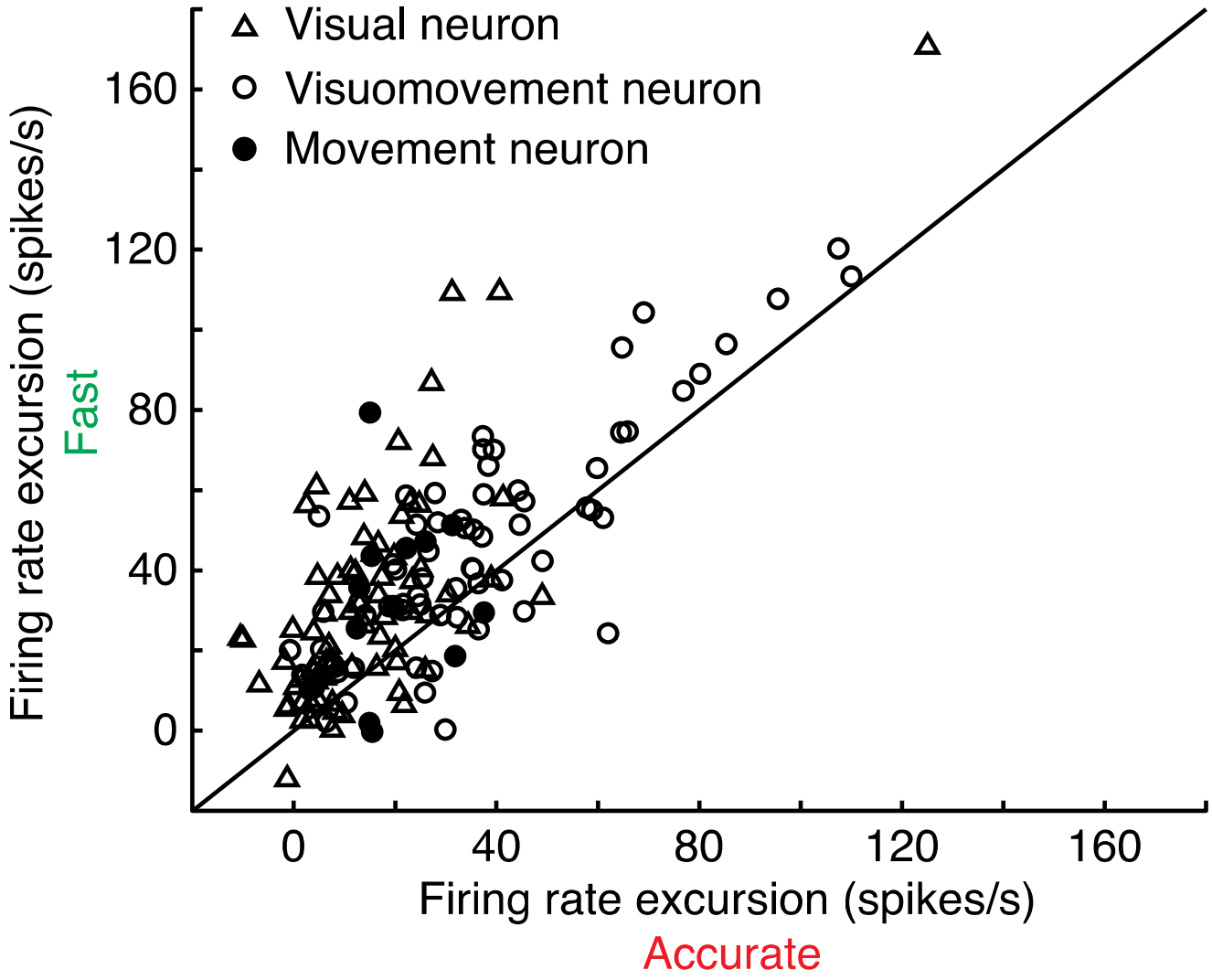

Figure S4. Firing rate excursion. For each neuron, we calculated the difference between average activity 20 – 10 ms prior to saccade and average activity in the 100 ms prior to array presentation. The excursion was significantly higher for the Fast condition as compared to the Accurate condition for all neuron types (Visual neurons: $t_{73} = -7.5$, $p < 0.001$; Visuomovement neurons: $t_{69} = -5.4$, $p < 0.001$; Movement neurons: $t_{13} = -2.1$, $p = 0.05$).

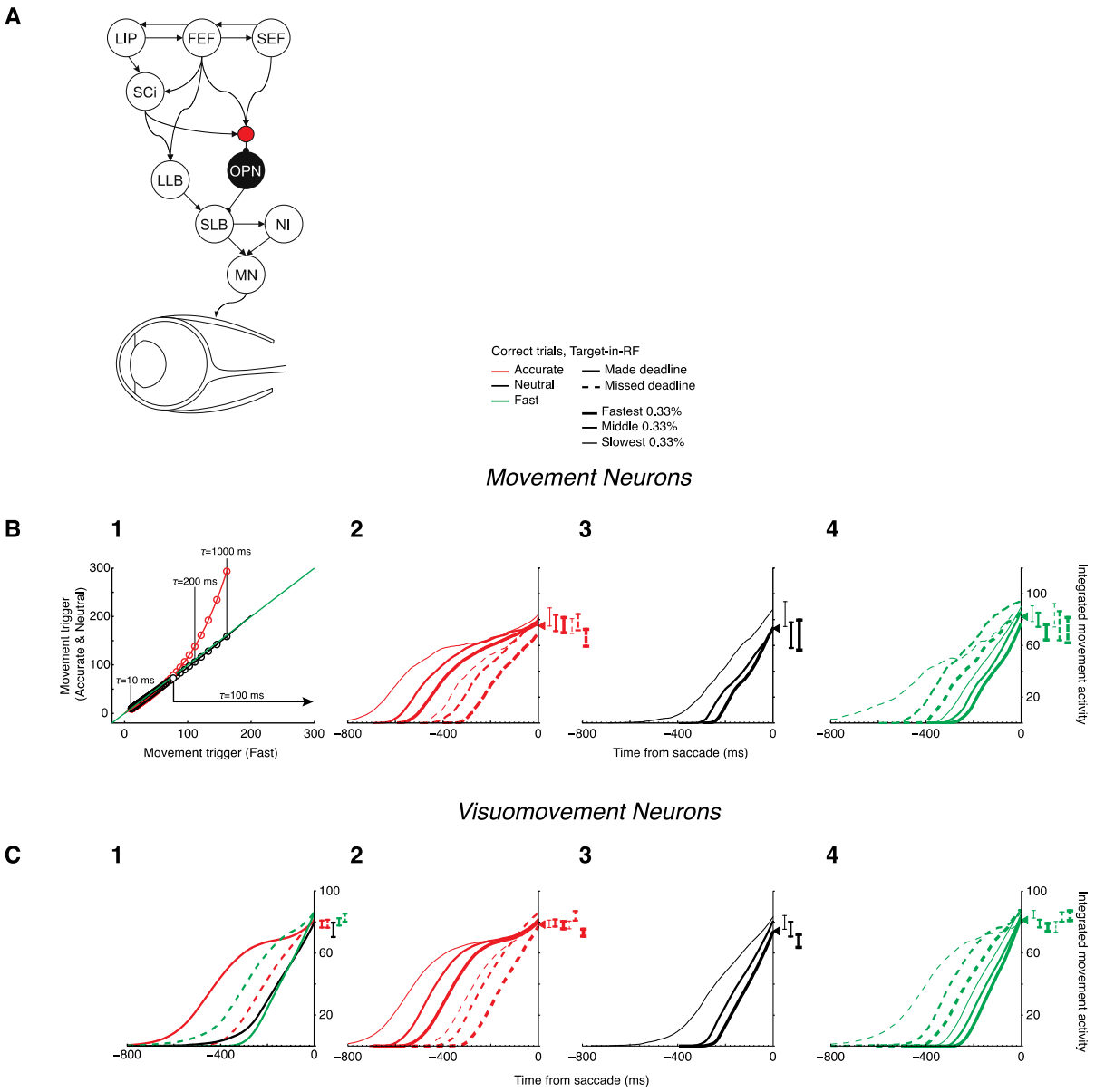

Figure S5. A, Diagram of key neurons, structures and connections that produce saccadic eye movements. The afferent visual pathway is not included. LIP, lateral intraparietal area; FEF, frontal eye field; SEF, supplementary eye field; SC_i, intermediate layers of superior colliculus; LLB, long lead burst neuron; OPN, omnipause neuron; SLB, short lead burst neuron; NI, neural integrator; MN, motor neuron. Saccades are initiated only when OPN are inhibited, represented by the red unit. This inhibition is a site of summation of influences from the FEF, SC, and SEF.

B, Integration of movement neuron activity. We explored the effect of integration time constant (τ) on the final value before saccade (**1**). For each τ the integrated value 20-10 ms before saccade initiation was measured for each SAT condition. Values from Accurate (red) and Neutral (black) conditions are plotted against values from the Fast condition. We submitted these trigger values to linear regression and found that trigger values between SAT conditions are invariant for time constants in the range $7.1 < \tau < 166.7$ ms. With $\tau = 100$ ms the time-course of integrated values are shown for Accurate (**2**), Neutral (**3**) and Fast (**4**) SAT conditions. Average integrated values divided into fastest (thick), intermediate (thinner) and longest (thinnest) RT quantiles with RTs distinguished by made (solid) and missed (dashed) deadlines. Triangles on ordinate mark mean integrated threshold within an SAT condition. Vertical bars reflect $\pm$1 SEM for each type of trial. None of the integrated values 20 – 10 ms before saccade were significantly different (linear regression).

C, Integrated visuomovement activity averaged for each SAT condition when conditions were made and missed (**1**, corresponding to Figure 5), and in RT quantiles for each SAT condition (**2-4**). Integrated visuomovement neuron discharge rates reach an invariant level 20 – 10 ms prior to saccade initiation (all $p > 0.05$, linear regression). The apparent plateau of activity during longer RT trials arises from averaging the visual responses inherent in visuomovement neurons.